# Investigations on the reciprocal ternary system (±)-2-phenylpropionic acid–(±)-α-methylbenzylamine. Impact of an unstable racemic compound on the simultaneous resolution of chiral acids and bases by preferential crystallisation† ‡

**Fabrice Dufour, Claire Gervais, Marie-Noëlle Petit, Guy Perez and Gérard Coquerel ***

*Unité de Croissance Cristalline et de Modélisation Moléculaire (UC²M²), UPRES EA2659, IRCOF, Université de Rouen, 76821 Mont-Saint-Aignan cedex, France*

***Received (in Cambridge, UK) 19th January 2001, Accepted 17th July 2001***
***First published as an Advance Article on the web 7th September 2001***

New studies on the reciprocal quaternary system (±)-2-phenylpropionic acid [(±)-**1**]–(±)-α-methylbenzylamine [(±)-**2**]–ethanol confirm the presence of a stable conglomerate (p and p′ salts), but polymorphism of the n salt as well as an unstable racemic compound have been detected. The kinetic parameters of the irreversible transformation of the unstable racemic compound into the stable conglomerate have been determined from experimental X-ray powder diffraction data. The simultaneous resolution of (±)-**1** and (±)-**2** by means of preferential crystallisation (auto-seeded process) of the stable pair of enantiomorphous salts, was achieved. However, the entrainment effect (given by the maximum enantiomeric excess of the counter enantiomer in the mother solution, reached at the end of the stereoselective crystallisation ($ee_{max}^{f}$ = 5.2%)) is limited. This is consistent with the existence of the unstable racemic compound, as accounted for in a recent model of molecular interactions occurring at the crystal–mother solution interface in the course of preferential crystallisation. An extended version of this model rationalises a kinetic advantage of the crystal growth rate of racemic compounds over the conglomerates as well as a large supersaturation capacity of the mother solution in such a reciprocal quaternary system (±)-acid, (±)-base and solvent.

## Introduction

Crystallisation processes are the most suitable techniques for the preparative resolution (*i.e.* separation) of the enantiomers of a racemic mixture:[1] (i) the diastereomeric salt formation (or classical resolution), relying on the difference of the physico-chemical properties of diastereomers, involves an active role of an intermediate optically active compound (the resolving agent). Nevertheless, the maximum theoretical yield is thermodynamically limited. (ii) The preferential crystallisation (PC) (or crystallisation by entrainment) consists of the alternate stereoselective crystallisation of a single enantiomer out of a quasi racemic mixture and, after each filtration, of the recycling of the mother liquor in order to crystallise the other enantiomer. The latter method is only applicable to racemic mixtures which crystallise as a conglomerate (*i.e.* a 50%–50% eutectic mixture of both enantiomers). Since only 5% to 10% of racemic mixtures crystallise as a conglomerate,[1a,b] tedious trial and error crystallisations of numerous derivatives in various solvents are often carried out to overcome this drawback and the lack of *a priori* indications of whether a given chiral compound crystallises as a conglomerate.

The first purpose of this study is to investigate another resolution process which combines the two methods stated

† Electronic supplementary information (ESI) available: examination of the crystal growth paths for racemic solutions and the case of non-racemic solutions—application to the PC. See http://www.rsc.org/suppdata/p2/b1/b100706h/

‡ **Glossary**: A Acidic ion. *A* Configuration of a ladder; the chiral ion(s) of the ion pair at the top has (have) the right absolute configuration. AS3PC Auto-seeded programmed polythermic preferential crystallisation. B Basic ion. *c* Concentration. $c_{sat}$ Concentration of a saturated solution. conglo Conglomerate. CCI Chiral counter-ion. DIPE Diisopropyl ether. $ee_{max}^{f}$ Maximum ee of the mother liquor at the end of the entrainment effect. *E* Percentage of rungs formed [= $(i - 2q)/i$]. $E_{P/N}^{hkl}$ Set of ratios of the homochiral (*R*–*R* or *S*–*S*) interaction energies over the heterochiral (*R*–*S*) interaction energies at the (*hkl*) crystal–mother liquor interfaces. $E(P_{i-2q}^{max})$ Most probable percentage of rungs formed. F0D2 Desorption mechanism (0 bonds are formed, 2 bonds are destroyed). F2D0 Adsorption mechanism (2 bonds are formed, 0 bonds are destroyed). F3D1 Insertion mechanism (3 bonds are formed, 1 bond is destroyed). $(F3D1)_n$ Succession of several F3D1 mechanisms. *i* Number of events. IPBC Ionic periodic bond chain. *j* Suffix which defines the columns of the triangular tables. *K* Equilibrium constant of the double decomposition reaction. *M* Configuration of a ladder; only one of the two chiral ions of the ion pair at the top has the right absolute configuration. n Salt composed of A(+)B(−) ion pairs (n also refers to a single ion pair A(+)B(−)). n′ Salt composed of A(−)B(+) ion pairs (n′ also refers to a single ion pair A(−)B(+)). *N* Configuration of a ladder; only one of the two chiral ions of the ion pair at the top has the right absolute configuration. NCCI Non-chiral counter-ion. OP Optical purity. p Salt composed of A(+)B(+) ion pairs (p also refers to a single ion pair A(+)B(+)). p′ Salt composed of A(−)B(−) ion pairs (p′ also refers to a single ion pair A(−)B(−)). PC Preferential crystallisation. $P_{i-2q}$ Probability of the formation of $i - 2q$ rungs, whatever the configuration (*A*, *M*, *N* or *Z*) of the ladder. *q* Integer number ranging from 0 to *i*/2, used to define the possible numbers of rungs formed for *i* events ($i - 2q$). rac Racemic compound. RA Relative advantage (of the racemic compound); [= $(E(P_{i-2q}^{max})_{rac} - E(P_{i-2q}^{max})_{conglo})/E(P_{i-2q}^{max})_{conglo}$]. $T_L$ Temperature of dissolution of the racemic mixture. $T_{homo}$ Temperature at which the whole mixture (partially enriched) is dissolved. $T_B$ Temperature of the starting point of the PC ($T_L < T_B < T_{homo}$). $T_F$ Temperature of filtration. $U_{ij}$ Values of the triangular tables. Probability of reaching the situation (*xX*) corresponding to the $j^{th}$ column of a triangular table when *i* events occurred. (*xX*) Situation of a ladder; *x*: number of rungs formed, *X* = *A*, *M*, *N* or *Z*. XRPD X-Ray powder diffraction. *Z* Configuration of a ladder; the chiral ion(s) of the ion pair at the top has (have) the wrong absolute configuration. *β* Supersaturation (= $c/c_{sat}$). Δ*E* Interval of *E* for which $\Sigma P_{i-2q} \geq 99\%$. π Ion pair $A_RB_R$ (π also refers to the salt composed of these pairs). π′ Ion pair $A_SB_S$ (π′ also refers to the salt composed of these pairs). ν Ion pair $A_RB_S$ (ν also refers to the salt composed of these pairs). ν′ Ion pair $A_SB_R$ (ν′ also refers to the salt composed of these pairs). $\Sigma P_{i-2q}$ Sum of the probabilities $P_{i-2q}$ for several possible numbers of rungs formed $i - 2q$.

 DOI: 10.1039/b100706h

above. This could allow chemists to reconsider most of the already established resolution processes *via* diastereomeric salt formation, particularly if the resolving agent is cheaply available in the racemic form. This process consists in resolving enantiomerically-related diastereomeric salts by entrainment and preferably by the auto-seeded process.[2] The main interest of this process is the simultaneous resolution of two racemic mixtures. Let us consider the reciprocal ternary system of a racemic base (±)B and a racemic acid (±)A. In the solid state and provided no solid solution exists, five crystalline (1 : 1) phases can potentially be formed: (+)A(+)B: p salt and (−)A(−)B: p′ salt, which are enantiomorphous salts, (+)A(−)B: n salt and (−)A(+)B: n′ salt, which are enantiomorphous salts and (±)A(±)B: racemic compound.

The heterogeneous equilibria of interest in this study consist of a 1 : 1 acid : base ratio stoichiometry and can be described by the reciprocal ternary subsystem of components: p, p′, n and n′ salts and where the double decomposition shown in reaction (1) can occur in the molten state.

$$A(+)B(+) + A(-)B(-) \rightleftharpoons A(+)B(-) + A(-)B(+) \quad (1)$$

If there is no racemic compound formation, one pair of salts (p–p′ for instance) is more stable than the other (n–n′), and, at least in a given range of temperature, the (1 : 1) mixture crystallises as a conglomerate. In this case, a resolution by entrainment can theoretically be achieved in the reciprocal quaternary system (±)A–(±)B–solvent. It consists of the alternate crystallisation of both enantiomorphous more stable salts (p and p′ in this case), out of a twofold quasi racemic mixture of four species, two of which (the less stable pair of salts) do not participate in the heterogeneous equilibria (instead of the usual alternate crystallisation of two enantiomers out of a simple quasi racemic mixture). Then, pure optical isomers of both the racemic acid and the racemic base are recovered by salting out each resolved enantiomorphous salt. As far as we know, resolution of enantiomorphous salts *via* crystallisation has already been achieved but always by means of seeding and/or without any successive recycling of the mother liquor.[3]

Leclercq *et al.* have already widely studied the heterogeneous equilibria involving the salts of 2-phenylpropionic acid (or hydratropic acid) (**1**) and α-methylbenzylamine (**2**) with or without ethanol. They have determined two experimental isotherms of the ternary system p salt, n salt, ethanol 96%, at 10 °C and 30 °C, showing that these salts crystallise as a eutectic mixture, p salt (and therefore p′ salt) having the lowest solubility.[4] They have also described the experimental condensed phase diagram of the reciprocal ternary system (±)-**1**–(±)-**2** as a stable conglomerate of p and p′ salts near the melting point (no double salt formation).[5] Therefore, basic thermodynamic requirements were met in the reciprocal quaternary system (±)-**1**–(±)-**2**–ethanol in order to achieve the simultaneous resolution by preferential crystallisation. Furthermore, in connection with these studies, Brianso[6] has determined the crystal structures of the p and n (later designated as n form I) salts by means of single crystal X-ray diffraction analyses.

However, two main problems can be expected: (i) the PC is carried out in a very hostile medium since the mother liquor contains more than 50% impurities (the counter enantiomer) at the end of the specific crystallisation. In the case of the simultaneous resolution, the selective crystallisation is expected to be even more difficult: although a racemic mother liquor contains two wrong constitutive units out of four (50% of wrong ions), there is only one right (1 : 1) combination (the crystallising ion pair) out of four possibilities; (ii) an additional difficulty can arise when there exists an unstable or metastable racemic compound. A model of molecular interactions occurring at the crystal–mother liquor interface during the PC has been proposed by Houllemare-Druot and Coquerel[7] to rationalise the impact of such a racemic compound on the entrainment effect.

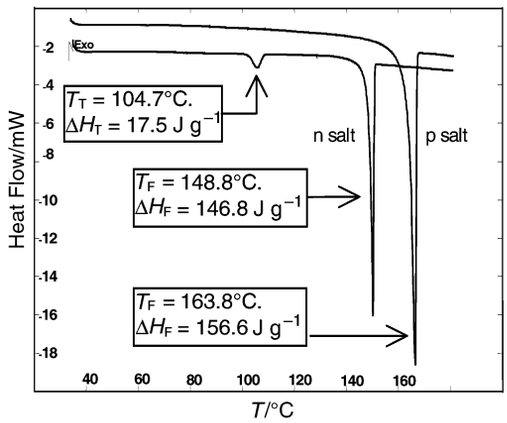


**Fig. 1** DSC analyses of n salt [(+)-**1**–(−)-**2**] and p salt [(+)-**1**–(+)-**2**]. Heating rate: 2 °C min$^{-1}$.

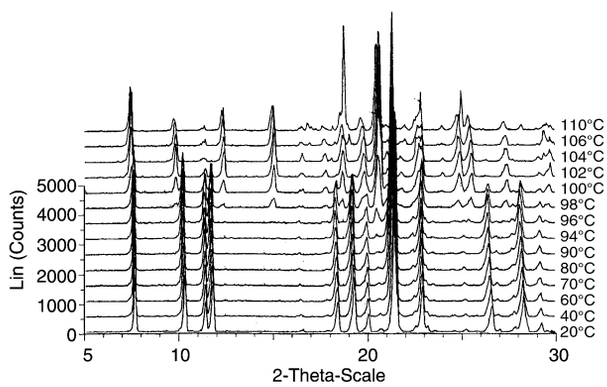


**Fig. 2** Temperature-resolved XRPD analysis of the n salt.

The second aim of this study is to extend the kinetic part of this model to a simple kinetic model of crystal growth of ammonium carboxylate salts. The case of pairs of reciprocal salts (*i.e.* anion and cation both chiral) is examined.

## Results

### Evidence of the n salt polymorphism and existence of an unstable racemic compound

Differential scanning calorimetry (DSC) analyses of pure n salt always display an endothermic phenomenon (at 105 °C) prior to melting (at 149 °C) (Fig. 1). The assumption of a polymorphic transition near 100 °C is confirmed by a temperature-resolved X-ray powder diffraction analysis (Fig. 2). The hypothesis of a desolvation is rejected since the X-ray powder diffraction pattern of the low temperature form corresponds to that of the non-solvated n salt structure determined by Brianso.[6] The low and high temperature forms are, from now on, called n salt form I and n salt form II respectively. We can assume that by contrast to Leclercq *et al.*,[4,5] a high chemical purity of the sample allowed us to detect this polymorphic transition.

An unstable racemic compound has been detected by fast cooling or by swift evaporation of an ethanolic solution of an equimolar mixture of (±)-**1** and (±)-**2**. Fig. 3 shows the experimental X-ray powder diffraction (XRPD) patterns of p salt, n salt form I, n salt form II and the unstable racemic compound. The calculated (from atomic positions determined by Brianso) XRPD patterns of p salt and n salt form I (also displayed on Fig. 3) match quite well with the experimental ones. Moreover, the crystallographic parameters obtained from the peak assignment of the experimental XRPD patterns are well fitted

**Table 1** Crystallographic parameters of the p salt, n salts form I and form II and the unstable racemic compound

| | p Salt | | n Salts | | | Racemic compound |
|---|---|---|---|---|---|---|
| | XRPD | Single crystal | Form I XRPD | Form I single crystal | Form II XRPD | XRPD |
| *a*/Å | 11.30(±0.05) | 11.211(±0.010) | 17.14(±0.05) | 17.080(±0.010)[a] | 17.60(±0.05) | 17.81(±0.05) |
| *b*/Å | 12.30(±0.05) | 12.249(±0.010) | 15.57(±0.05) | 15.470(±0.010) | 15.53(±0.05) | 6.06(±0.05) |
| *c*/Å | 6.56(±0.05) | 6.558(±0.010) | 5.82(±0.05) | 5.800(±0.010) | 5.97(±0.05) | 15.23(±0.05) |
| $\gamma$/° | 116.0(±0.05) | 115.84(±0.05) | 90 | 90 | 90 | 97.1(±0.05) |
| *V*/Å$^3$ | 818 | 810 | 1554 | 1532 | 1631 | 1631 |
| *Z* | 2 | 2 | 4 | 4 | 4 | 4 |
| *M(N)* or *R* | 15.0 (21) | 0.074 | 17.0 (11) | 0.078 | 20.1 (22) | 12.3 (20) |
| $\rho$/g cm$^{-3}$ | 1.10 | 1.11 | 1.16 | 1.18 | 1.10 | 1.10 |
| Space group | Compatible $P2_1$ | $P2_1$ | Compatible $P2_12_12_1$ | $P2_12_12_1$ | Compatible $P2_12_12_1$ | Compatible $P2_1/b$ |

[a] Value extracted from the Cambridge Structural Database System.

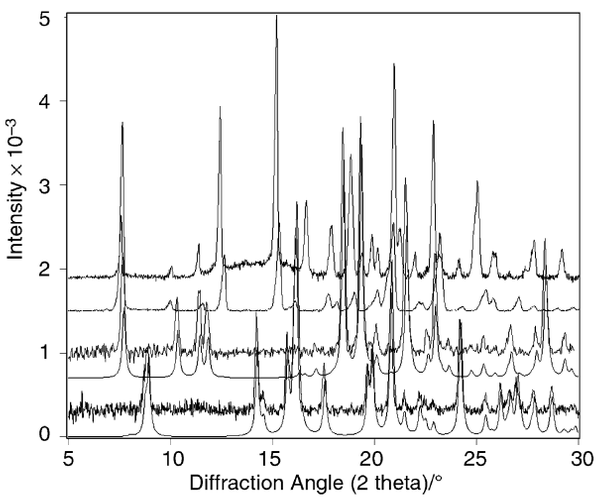


**Fig. 3** Experimental (and calculated) XRPD patterns of α-methylbenzylammonium hydratropate salts. From bottom to top: p salt (calculated), p salt (exp.), n salt form I (calculated), n salt form I (exp.), n salt form II (20 °C), unstable racemic compound. The experimental patterns of p salt and n salt form I were performed with the capillary set-up in order to avoid strong preferential orientation effects.

to those determined by single crystal X-ray diffraction analysis (Table 1). However, provided that good quality single crystals can be obtained, single crystal X-ray diffraction analyses of n salt form II and the unstable racemic compound should be worth conducting to confirm the results of the peak assignment of their XRPD patterns. Nevertheless, the clear analogies of the XRPD patterns tend to show that n salt form II and the unstable racemic compound have rather similar crystalline structures.

### Kinetics of the irreversible transformation of the unstable racemic compound into the stable conglomerate

An X-ray powder diffraction experiment monitoring the annealing of the unstable racemic compound at 70 °C for 80 hours shows an irreversible transformation of the sample into the stable p–p′ conglomerate (Fig. 4). The exponential-like decay of the unstable racemic compound prompted us to assume that it is a first order kinetics transformation, diffusion and/or interface controlled. Assuming that the Eyring's theory equations of the transition state[8] are valid, two other annealing experiments at 50 °C and 60 °C allowed the calculation of the activation energy and the kinetic parameters (Table 2) of this irreversible solid–solid transformation by means of eqns. (2)–(5). The negative sign of the activation entropy ($\Delta S^{\ddagger} \approx$ $-9$ J K$^{-1}$ mol$^{-1}$) is worth noting, as it means that the activation state is more ordered than the initial racemic compound. This is consistent with the molecular discrimination which must occur to form both enantiopure crystals starting from the racemic compound.

$$\mathrm{d}c/\mathrm{d}t = kc \quad (2)$$

$$k = A \exp(-E_A/RT) \quad (3)$$

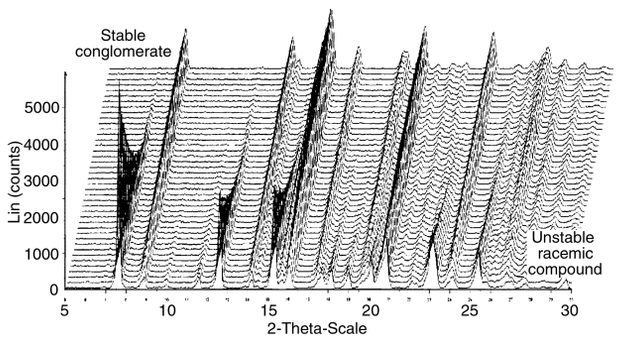


**Fig. 4** Annealing of the unstable racemic compound at 70 °C monitored by XRPD. Measurement duration: 40 min, time interval between two measurements: 60 min.

$$k = k_B T K^{\ddagger}/h \quad (4)$$

$$\Delta G^{\ddagger} = -RT \ln K^{\ddagger} \quad (5)$$

### Simultaneous resolution

**Basic principles of the AS3PC process.**[2] Fig. 5 displays the typical pathway of the solution point $S_E$ during a single run of the so-called auto-seeded programmed polythermic preferential crystallisation (AS3PC). This process can briefly be described as follows.

(i) The starting point is a partially enantiomerically enriched mixture of enantiomers plus solvent (*i.e.* the quasi-racemic solution represented by point *E* on the upper projection of Fig. 5), held a sufficient time at $T_B$, a temperature at which a saturated solution (represented by point $S_E$) is in equilibrium with pure crystals of the enantiomer in excess (*R* for instance). $T_L < T_B < T_{homo}$ where $T_L$ is the temperature of dissolution of the whole racemic mixture only, and $T_{homo}$ the temperature at which the whole mixture (partially enriched) is dissolved.

(ii) An adapted cooling program is applied to the system, allowing the *R* crystals to grow and keeping the solution supersaturated with regard to the opposite enantiomer (*S* in this case). The point representing the solution then evolves from $S_E$ at $T_B$ to $F_A$ at $T_F$, close to the stable (up to $T_L$) and metastable (down to $T_L$) solubility curves depicted on the isoplethal section Y–R.

(iii) The suspension is filtered off to separate the mother liquor from *m* grams of *R* enantiomer (according to the lever rule $m = m_t(F_A E/F_A R)$ applied on the segment YR of the upper projection (in mass fraction); where $m_t$ is the total mass of the system).

**Table 2** Kinetic parameters of the solid–solid transformation of the unstable racemic compound into the stable conglomerate

| $T$/K | 323 | 333 | 343 |
|---|---|---|---|
| $10^6\ k/s^{-1}$ | 1.203 | 4.506 | 14.190 |
| Mean $E_A$/kJ mol$^{-1}$ | | +113.5 | |
| Mean $A/s^{-1}$ | | $6.14 \times 10^{12}$ | |
| $\Delta H^{\ddagger}$/kJ mol$^{-1}$ | +110.9 | +110.8 | +110.7 |
| $\Delta S^{\ddagger}$/J mol$^{-1}$ K$^{-1}$ | −9.1 | −9.3 | −9.6 |

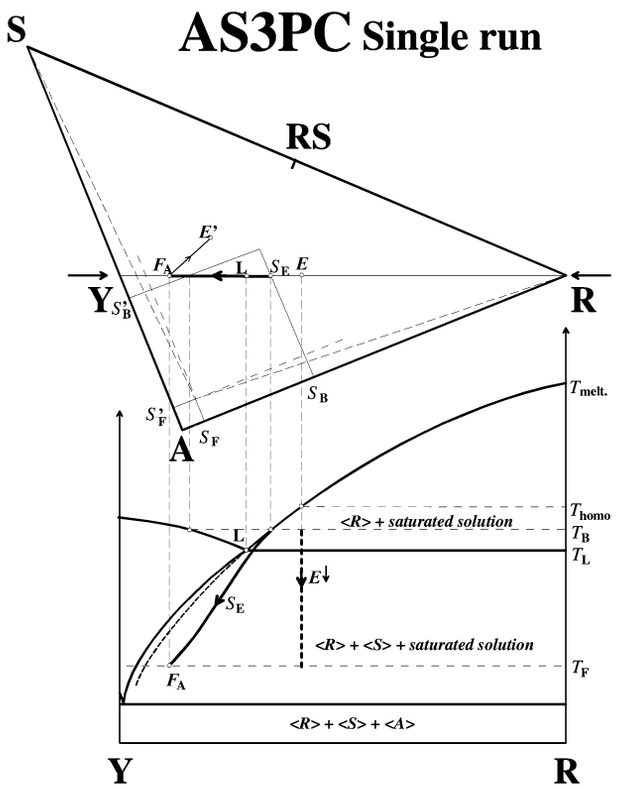


**Fig. 5** Pathway of the solution point $S_E$ in the course of a single run of AS3PC, displayed on the isoplethal section RY$T$ of the equilibrium phase diagram. On the upper part of the figure, the pathway of $S_E$ is projected along the $T$ axis, on the isothermal sections at $T_F$ and $T_B$. $S_B$ and $S_F$ are the solubilities of the enantiomer $R$ in the solvent A at $T_B$ and $T_F$ respectively ($S'_B$ and $S'_F$ are the same values for the enantiomer $S$). In bold italics: coexisting phases if the system is in equilibrium. $F_A$ is the actual (or practical) limit of the entrainment. The system reaches an equilibrium state at $T_B$ and then is out of equilibrium during the crystallisation.

(iv) $m$ Grams of racemic crystals are added to the mother liquor so that the system is now represented by the point $E'$ (symmetrical to the point $E$ with reference to the (A,RS,$T$) plane).

(v) By applying the steps (i) to (iv) to this mixture (now enriched in the $S$ enantiomer) the starting point ($E$) is recovered and further cycles of alternate crystallisation of both enantiomers can be performed by means of the same procedure.

**Results of the preferential crystallisation.** The thermodynamic characteristics of the system are as follows.

(i) Concentration of the racemic mixture of p and p′ salts in the solution (owing to the definition in the Experimental section): $c(\pm\pm) = 17.5\%$.

(ii) Temperature of dissolution of the racemic mixture: $T_L = 22.7$ °C.

(iii) Evolution of $T_{homo}$ with the ee of the solution at constant $c(\pm\pm) = 17.5\%$: Table 3.

Classical resolution of (±)-**1** by means of optically active α-methylbenzylamine (+)-**2** in ethanol was previously performed to get pure p salt (without any n salt crystals as impurity). Then an equimolar mixture of (±)-**1** and (±)-**2** was enantiomerically enriched (5–6% ee) by using this salt, to perform the PC of p and p′ salts at a 50 ml scale. 17 runs were implemented with the average results reported in Table 4. Several runs were also performed at a 160 ml scale to collect a sufficient quantity of enantiomerically enriched mixture of p and p′ salts so that the scale-up of this resolution process to 2 litres could be investigated.

**Table 3** Evolution of $T_{homo}$ with the ee of the solution at constant $c(\pm\pm) = 17.5\%$

| ee (%) | $T_{homo}$/°C |
|---|---|
| 0.0 | 22.7 |
| 2.0 | 25.2 |
| 4.0 | 27.4 |
| 6.0 | 28.8 |

Assuming that $N - 1$ runs were already performed, these are the different steps of run $N$ (Fig. 6): the composition of the mother solution obtained after the filtration of run $N$ was determined by means of polarimetry and refractive index measurement *via* the calibration method described in the Experimental section. Ethanol first, and then both liquids (±)-**1** and (±)-**2** were added to that mixture in order to recover the starting $c(\pm\pm)$, whatever the $ee^f_{max}$ reached at the end of run $N$. The homogeneous mother solution remained clear. The *in situ* crystallisation of the conglomerate was initiated by seeding the solution at 22 °C with 0.3 g of conglomerate (±±) crystals previously crystallised and sieved (≤200 μm), and cooling this clear suspension down to 8 °C owing to an adapted cooling program. This preliminary step, prior to the stereoselective crystallisation, allows the *in situ* salt formation (p–p′) avoiding the undesired unstable racemic compound crystallisation. Then the obtained slurry was heated up to and maintained at $T_B = 23.8$ °C for 1 hour so that the stereoselective dissolution ensures the thermodynamic equilibrium of the pure crystals of p (or p′) salt with the mother solution (the auto-seeding). The stereoselective crystallisation was induced by another adapted cooling down to 8 °C, and monitored by polarimetry and refractive index measurements *via* the calibration method already mentioned. An isothermal filtration was implemented on a glass filter No. 3 thermostatted at 8 °C. The crops were washed twice with 80 ml of cold diisopropyl ether (DIPE) and dried at 75 °C. The results are displayed in Table 5. All these crystallisations were monitored by means of the focused beam reflectance measurements (FBRM).[9] The information obtained from this technique is the real-time evolution of the chord length distribution. A chord length is a straight line between any two points on the edge of a particle and what is measured here must not be assimilated to the crystal size distribution. Up to run 7, we tried to improve the OP of crops by filtering the crystals off before any significant increase of the number of small chords (which could have meant that the nucleation of either the counter enantiomer or the unstable racemic compound had begun). But, despite the drop in both the mass of crude crops and $ee^f_{max}$, the OP of crops did not significantly improve. A smoother cooling program was tested during run 7. Although the OP of the crops has been improved (87%), the crystallisation was too slow and for an equivalent crystallisation duration (111 min), the $ee^f_{max}$ dropped (4.5%). From run 8 onwards, a lower maximum stirring rate was tested, inducing a longer duration of the experiment.

Crude crops obtained from odd runs on the one hand, and even runs on the other hand, were mustered. As the pair of p–p′ salts crystallises as a stable conglomerate, enantiopurification was achieved by means of recrystallisation of these salts. The recovery of (+)-**2** and (−)-**2** was not carried out. The results of purification and salting out of p and p′ salts are collected in Table 6. The detailed procedures are depicted in the Experimental section.

**Table 4** Average results of the preferential crystallisation of p and p′ salts at a 50 ml scale (17 consecutive runs)

| Mass of crude crop/g | Optical purity (OP) (%) | Mass of pure enantiomer/g | $ee^{f}_{max}$ (%) |
|---|---|---|---|
| 0.82 | 85.7 | 0.70 | 5.5 |

**Table 5** Results of the preferential crystallisation of p and p′ salts at a 2 L scale—the starting $c(\pm\pm) = 17.5\%$ of each crystallisation corresponds to 297 g of racemic mixture of p and p′ salts (164.4 g of (±)-**1** and 132.6 g of (±)-**2**) and 1400 g of ethanol

| Run | $T_B$/°C (stirring rate/rpm) | Maximum stirring rate/rpm (*t*/min) | Duration of crystallisation/min | Mass of crude crop/g | OP of the crops (%) | Mass of pure enantiomer/g | $ee^{f}_{max}$ (%) |
|---|---|---|---|---|---|---|---|
| 1 | 23.8 (200) | 250 (65) | 82 | 43.0 | 75.4 | 32.4 | 6.4 |
| 2 | 23.8 (200) | 275 (75) | 88 | 35.9 | 83.7 | 30.0 | 5.3 |
| 3 | 23.7 (200) | 250 (61) | 87 | 36.0 | 84.0 | 30.2 | 5.4 |
| 4 | 23.7 (200) | 250 (46) | 86 | 32.8 | 84.3 | 27.6 | 5.0 |
| 5 | 23.7 (200) | 250 (57) | 90 | 31.5 | 85.5 | 27.0 | 5.0 |
| 6 | 23.8 (200) | 250 (59) | 100 | 31.3 | 84.6 | 26.5 | 4.8 |
| 7[a] | 23.3 (200) | 250 (65) | 111 | 29.4 | 87.0 | 25.6 | 4.5 |
| 8 | 23.3 (180) | 240 (92) | 106 | 30.4 | 84.5 | 25.7 | 4.9 |
| 9 | 23.4 (180) | 200 (45) | 108 | 35.9 | 76.5 | 27.5 | 5.4 |
| 10 | 23.4 (180) | 220 (81) | 110 | 34.2 | 82.6 | 28.2 | 5.2 |
| 11 | 23.3 (180) | 220 (79) | 117 | 35.2 | 81.3 | 28.6 | 5.3 |
| 12 | 23.3 (180) | 220 (81) | 126 | 36.5 | 77.2 | 28.2 | 5.2 |
| 13 | 23.3 (180) | 220 (80) | 127 | 35.0 | 80.2 | 28.1 | 5.2 |
| Average | — | — | 103 | 34.4 | 82.1 | 28.2 | 5.2 |

[a] A different cooling program was tested during this run.

**Table 6** Recrystallisations and salting out of p and p′ salts

| Recrystallisations | | | | Salting out | | | |
|---|---|---|---|---|---|---|---|
| Salt | Mass/g (Average OP (%)) | Mass of pure salt/g | Yield (%)[a] | Enantiomer | Mass/g | ee (%) | Yield (%)[c] |
| p (++) | 201.1 (82.7) | 155.9 | 93.7 | (+)-**1** | 78.3 | >98 | 90.7 |
| p′ (−−) | 200.2 (80.6) | 137.3 | 85.1 | (−)-**1** | 70.6 | >99[b] | 92.9 |

[a] Global yield of recrystallisations, based on the amount of pure salt contained in the crude crops (*i.e.* based on mass of crude salt × OP). [b] The enantiomeric excess of the liberated acid was determined by HPLC analysis (Daicel chiralpack AD, 250 mm × 4.6 mm, heptane–isopropanol–trifluoroacetic acid: 92 : 8 : 1, 1 ml $min^{-1}$, $\lambda = 230$ nm). [c] Based on the amount of acid contained in the pure salt obtained after recrystallisations.

## Discussion

The magnitude of the entrainment effect (evaluated from the value of the final enantiomeric excess of the counter enantiomer in the mother solution at the end of each run of preferential crystallisation), was limited to an average value of $ee^{f}_{max} = 5.2\%$. These results match a model of molecular interactions occurring at the crystal–mother solution interface in the course of PC when there exists an unstable or metastable racemic compound.[7] This model, based on the crystal structure analogies of both the enantiomer and the unstable racemic compound of α-methylbenzylammonium chloroacetate salts, can be briefly described as follows. Let us define $\{E^{hkl}_{P/N}\}$ as the set of ratios of the homochiral (*R*–*R* or *S*–*S*) interaction energies over the heterochiral (*R*–*S*) interaction energies at the (*hkl*) crystal–mother liquor interfaces. The existence of a metastable or an unstable racemic compound brings qualitative evidence that $\{E^{hkl}_{P/N}\}$ contains several ratios slightly differing from 1. Furthermore, in the course of the PC, the non-crystallising enantiomer becomes predominant in the mother liquor so that the probability of heterochiral (*R*–*S*) interactions becomes greater than the probability of *R*–*R* (or *S*–*S*) docking at such interfaces. As the entrainment proceeds, the more the counter enantiomer is in excess in the mother liquor (so, at the end of the entrain-

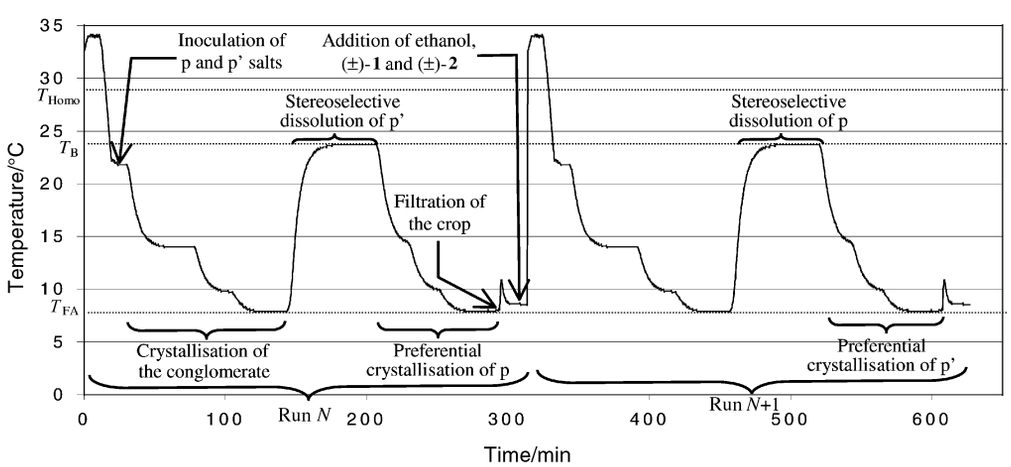


**Fig. 6** Cooling programs applied to the system during one cycle of crystallisation (2 runs).

ment, the more $ee^{f}_{max}$ increases), the more the stereoselective crystallisation is hindered at (*hkl*) interfaces with $E^{hkl}_{P/N} \approx 1$. Thus, by reversing the proposition, a poor $ee^{f}_{max}$ is likely to correspond to the limit of the entrainment effect when there exists a metastable or an unstable racemic compound.

In addition to this unfavourable set of energy ratios, this model proposes a rationalisation of the kinetic advantage of the nucleation and the crystal growth rates of the unstable racemic compound over the stable conglomerate. Here is an extended version of this model, suitable to account for this kinetic advantage when both the acid and the base are chiral (*i.e.* in the case of a pair of reciprocal salts).

### Kinetic model of crystal growth of chiral ammonium carboxylate salts composed of "ladder-shaped" ionic periodic bond chains (IPBC) in a racemic (or close to racemic) solution

**Notations.** (i) Carboxylate and ammonium ions are respectively symbolised as A and B. A subscript *R* or *S* indicates their absolute configuration if necessary. (ii) Hereafter, unlike the usual naming of diastereomeric salts (based on the sign of the optical rotation of the starting molecules), π and π′ stand for $A_RB_R$ and $A_SB_S$ respectively, and ν and ν′ stand for $A_RB_S$ and $A_SB_R$ respectively. (iii) These letters stand for either the salts or the ion pairs they are composed of.

**Introduction.** In the crystal structure of the enantiomer of α-methylbenzylammonium chloroacetate salt, ion pairs are arranged around a twofold screw axis and form strong ionic periodic bond chains (strong IPBC) which can be schematised as "ladders"[7] (Scheme 1). In the crystal structure of the unstable racemic compound of these salts, similar "ladder-shaped" IPBCs exist, resulting from syndiotactic arrangements of both enantiomers.

In the crystal structure of the less soluble α-methylbenzylammonium hydratropate salts[6] (ν and ν′ salts according to the notations described above) similar ion pair packings also form "ladder-shaped" IPBCs. This kind of packing seems to frequently occur in ammonium carboxylate salts.[10] Assuming that the crystal structure of the unstable racemic compound is made up of such a syndiotactic arrangement of enantiomeric ion pairs, involving such IPBCs, an enhanced version of this model is proposed to: (i) evaluate the kinetic advantage of the crystal growth of the unstable racemic compound over the conglomerate starting from a twofold racemic solution of a chiral acid and a chiral base; (ii) compare this kinetic advantage of the racemic compound between chiral and non-chiral counter ion; (iii) assess the supersaturation capacity of the mother liquor during the crystallisation of the stable pair of diastereomeric salts, compared to that during the crystallisation of salts with a common achiral counter ion; (iv) examine the influence of an enantiomeric excess on these kinetics of crystal growth with the aim of reproducing the conditions of the PC. It is noteworthy that this kinetic model is applicable to any ammonium carboxylate salt with such ladder shaped IPBCs. However, some salts (with mandelic acid derivatives for instance) often display one additional hydrogen bond linking these IPBCs to each other. This is not considered in this model.

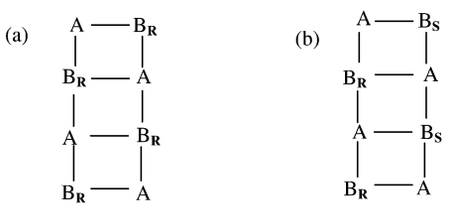


**Scheme 1** Schematic representation of a ladder-shaped IPBC found in α-methylbenzylammonium chloroacetate salts. (a) Enantiomer. (b) Racemic compound.

**Basic principles of the model.** The axes of these IPBCs usually correspond to the crystallographic direction of fastest crystal growth rate.[7,11] So, the adsorption and desorption mechanisms occurring at these IPBCs (*i.e.* at the top of the "ladders") are investigated in order to rationalise and compare the crystal growth kinetics. The solution is supersaturated ($\beta = c/c_{sat} > 1$) and crystals are growing *via* ion pair adsorption at the top of the ladders (see F2D0 mechanism below). As two (in the case of non-chiral counter ions (NCCI)) or four (in the case of chiral counter ions (CCI)) ion pairs exist in the mother solution, an adsorbed ion pair can contain one (or even two in the case of CCI) ion(s) whose absolute configuration is not that required. In this case, we examined the simplest way for the crystals to grow *i.e.* the schematic and elementary mechanisms necessary to evolve towards the right situation where both adsorbed ions have the right absolute configuration.

*Schematic mechanisms involved.* Three basic mechanisms are involved (Scheme 2).

The adsorption mechanism (called F2D0 because 2 bonds are formed and 0 destroyed).

The desorption mechanism (called F0D2 because 0 bonds are formed and 2 are destroyed).

The insertion mechanism (called F3D1 because 3 bonds are formed and 1 is destroyed) which results in the insertion of

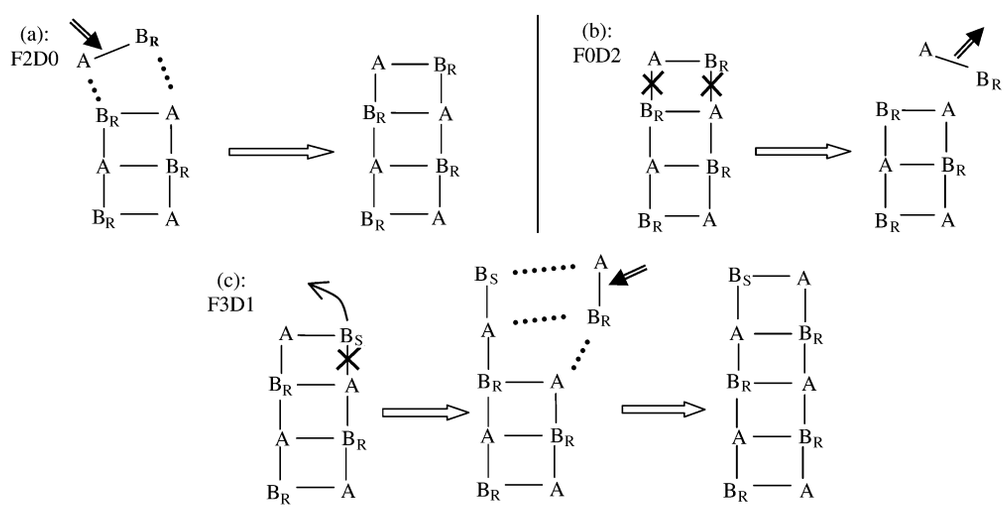


**Scheme 2** Schematic representation of the basic mechanisms involved during the crystal growth of chiral salts. (a) Adsorption (or F2D0) mechanism. (b) Desorption (or F0D2) mechanism. (c) Insertion (or F3D1) mechanism. F*x*D*y* means that *x* bonds are formed and *y* bonds are destroyed during the mechanism. A double arrow symbolises the moving of an ion pair.

one ion pair in the IPBC. In Scheme 2(c), the whole 3D environment of the chiral ion of the inserted pair is directly formed. As a consequence, a F3D1 mechanism exhibits a strong discriminating character.

As the activation energy of a mechanism is directly related to the number of bonds destroyed, the F3D1 mechanism is kinetically favoured since only one strong bond has to be broken (compared to two during F0D2 mechanism).

*Justification of the basic hypotheses.* The crystal grows by adsorption of ion pairs (and not of single ions). The solution is supersaturated ($\beta > 1$), the solvation capacity is exceeded and the ion pair dissociation is not very probable (particularly if the solvent is only slightly polar). However, we are dealing with molecular mechanisms (which belong to the thermodynamics of irreversible processes[12]) and the global macroscopic supersaturation ($\beta_{bulk}$) has to be distinguished from the local anisotropic supersaturation at the crystal–mother solution interfaces ($\beta_{loc}$): (i) the energy released by the formation of bonds tends to increase the local temperature (effect: $\beta_{loc}$ tends to decrease); (ii) attraction or repulsion phenomena of molecules at those interfaces[13] also play a role in $\beta_{loc}$ value. But this effect is most probably attractive at such interfaces where the IPBCs protrude (and therefore where the ionic groups of the crystallising units are readily accessible) so that $\beta_{loc}$ tends to increase. These two effects are antagonist but the acicular habit of crystals facilitates both the renewal of the solution and the heat dissipation (*via* the convection movements of the mother solution). Finally $\beta_{loc(IPBC)}$ is likely to be greater than $\beta_{bulk}$. Therefore, the small probability of the ion pair dissociation (due to the supersaturation state and therefore the exceeded solvation capacity of the solvent) is very likely at the local level.

The exchange of one ion at the top of the IPBC with one ion of a pair in solution could be contemplated (Scheme 3). But the insertion of the pair *via* F3D1 followed by the desorption of the "superficial" one (*i.e.* the pair remaining at the top of the ladder) *via* F0D2 leads to the same result. The main advantages of this two step description is (i) that the desorption (F0D2) is not always necessary since another F3D1 mechanism can be added up: ((F3D1)$_n$ mechanism (Scheme 4)); (ii) in the course of each mechanism, each ion remains bound with at least one counter-ion. Thus, no free ion is involved, as postulated first.

The crystal growth of a perfect single crystal is considered: no structural default of any kind is taken into account. Therefore, if a wrong ion is buried inside the crystal (Scheme 5), the constraints resulting from the unfavourable three dimensional environment of this ion involve the desorption of the superficial pair.

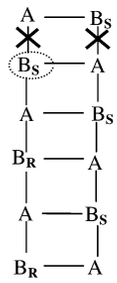

**Scheme 5** The absolute configuration of the buried ammonium ion (circled) is not that required. The superficial pair must be desorbed.

**Kinetic advantage of the crystal growth of the racemic compound.** *The case of a non-chiral counter ion (case of α-methylbenzylammonium chloroacetate salts).* According to the previous assumptions, Organisation charts 1 and 2 describe the possible ways for a crystal to grow, respectively in the case of the conglomerate and in the case of the racemic compound.

In the case of the racemic compound, when a wrong enantiomer is adsorbed, the insertion of the right enantiomer *via* F3D1 directly leads to the level $x + 2$ (Scheme 6). Then each of the two enantiomeric pairs can be adsorbed again.

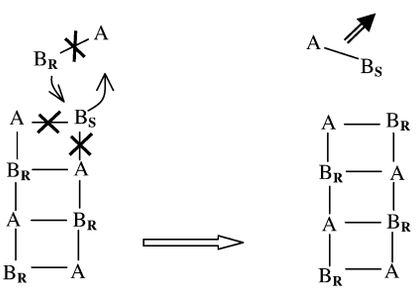

**Scheme 3** Potential F3D3 mechanism of exchange of one ion of the IPBC with one ion of a pair in solution.

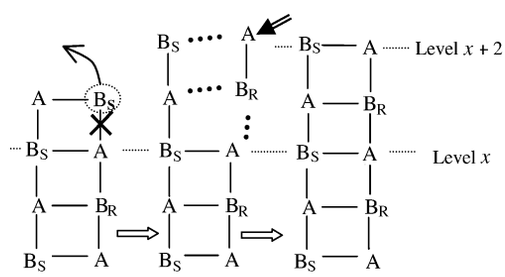


**Scheme 6** F3D1 mechanism leading to the formation of two right "rungs". The ion initially of wrong absolute configuration (circled), is in its right position after the insertion. (Here is the case of the racemic compound of a salt with a chiral counter ion.)

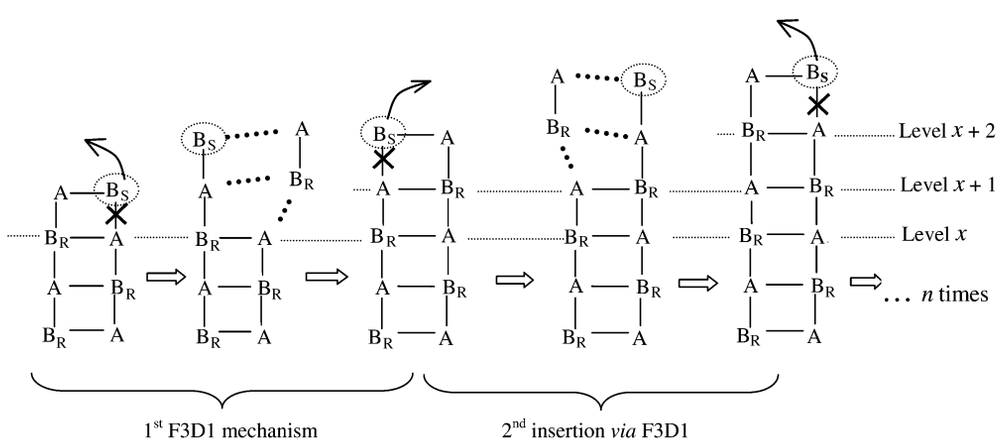


**Scheme 4** (F3D1)$_n$ mechanism. The ion of wrong absolute configuration is circled. (Here is the case of a conglomerate with NCCI.)

In the case of the conglomerate, on the surface of any crystal, when a wrong enantiomer is adsorbed, the insertion of the right enantiomer *via* F3D1 simply leads to the level $x + 1$ with a wrong pair remaining at the top. The crystal growth is therefore impaired since either the right enantiomers are sorted out and inserted *via* $(F3D1)_n$ (Scheme 4), or the superficial wrong pair is desorbed *via* F0D2. In the latter case, the next step can be the adsorption of each of the two enantiomeric pairs. In addition to this advantage in terms of activation energy of the desorption steps, the racemic compound is also favoured in terms of diffusion. In the case of the conglomerate, a wrong enantiomer desorbed from the surface has to migrate to another crystal (of the counter enantiomer) whereas in the case of the racemic compound, each of the IPBCs of each crystal is likely to adsorb both ion pairs so that the free migration path is in the magnitude of the molecular length.

*The case of a chiral counter ion (case of α-methylbenzylammonium hydratropate salts).* Two types of conglomerate can be contemplated: π–π′-type conglomerate (50 : 50% eutectic mixture of π salt and π′ salt crystals) or ν–ν′-type conglomerate (50 : 50% eutectic mixture of ν and ν′ salt crystals). Two ladder-shaped packings can also be contemplated for the racemic compound structure: either alternate "rungs" of π and π′ pairs (π-type racemic compound) or alternate "rungs" of ν and ν′ pairs (ν-type racemic compound) along the "ladder" (Scheme 7). Whatever the type of conglomerate on the one hand, and the type of racemic compound on the other hand, similar organisation charts can be drawn, leading to the same conclusions. It is noteworthy that other possible arrangements of ion pairs (ν–ν–ν′–ν′–ν–ν–ν′–ν′ . . . for instance) are not considered here.

The Organisation charts 3 and 4 (for π salt forming conglomerate and ν-type racemic compound respectively) display how a crystal can grow at a lower cost in activation energy when a "wrong" pair is adsorbed at the top of a ladder-shaped IPBC. In both cases (conglomerate and racemic compound), at each step of the crystal growth, among the four existing ion pairs in the solution (π, π′, ν and ν′ pairs), only one is composed of two

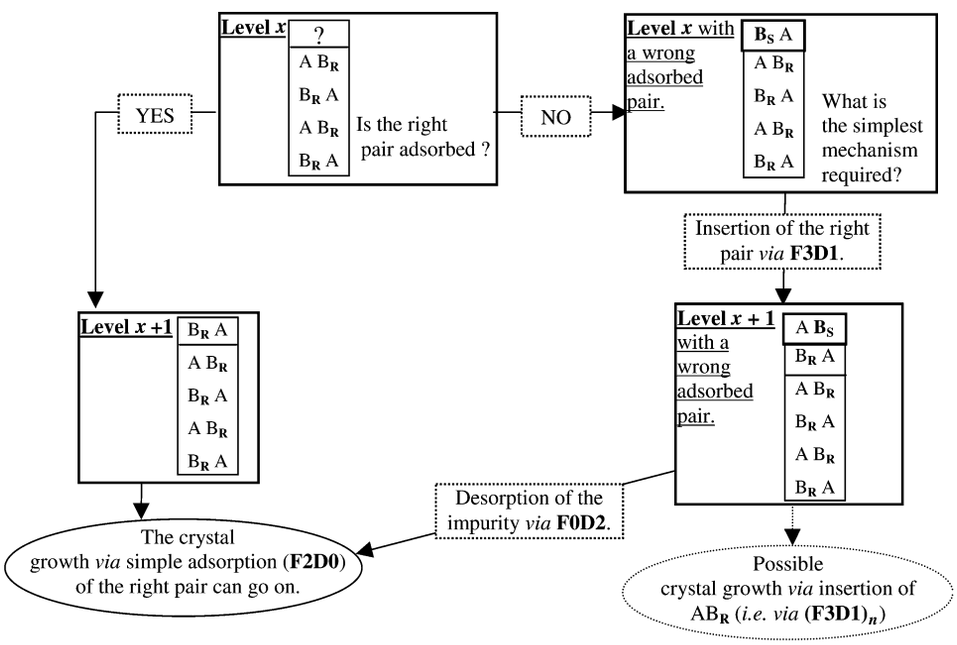


**Organisation chart 1** Crystal growth of the conglomerate in the case of a non-chiral counter ion.

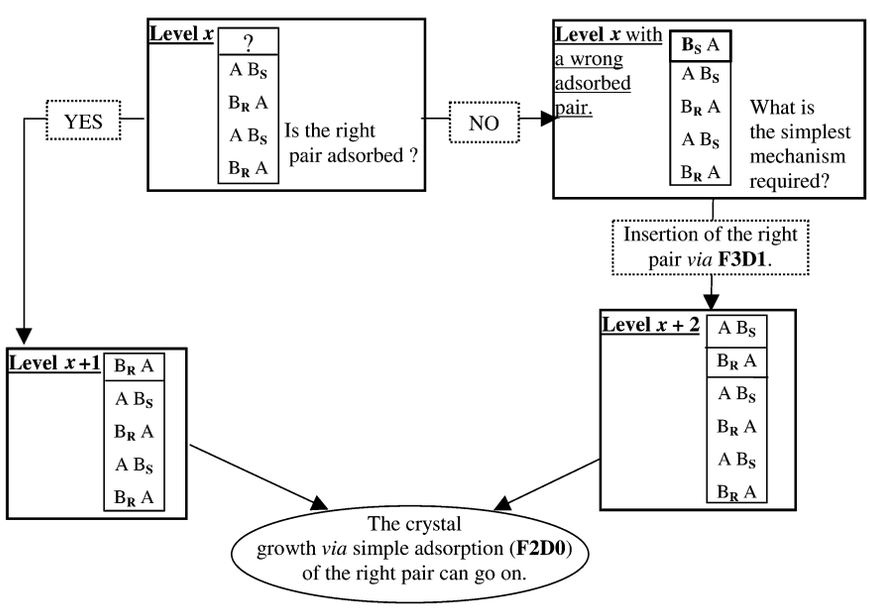


**Organisation chart 2** Crystal growth of the racemic compound in the case of a non-chiral counter ion.

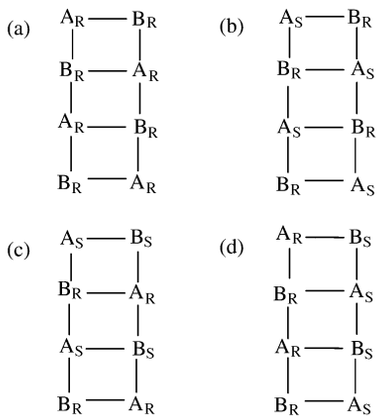


**Scheme 7** Schematic representation of the ladder-shaped IPBCs in the crystal structure of: (a) π salt (π–π′-type conglomerate); (b) ν′ salt (ν–ν′-type conglomerate); (c) π-type racemic compound; (d) ν-type racemic compound.

ions of required absolute configurations. There is also one pair whose both constitutive ions have a "wrong" absolute configuration: when such a pair is adsorbed, it must be entirely desorbed to let another pair be adsorbed in its place. The two other pairs have one ion of right absolute configuration only. When such a pair is adsorbed the situation is akin to that of a common non-chiral counter ion and a kinetic advantage of the racemic compound arises. The insertion of the right pair (π pair in the case of π salt or ν′ pair at level $x$ of the racemic compound growth (see Organisation chart 4)) leads to the formation of one right rung, the impurity remaining at the top (level $x + 1$ with an impurity at the top of the IPBC). The crystal growth can proceed *via* (F3D1)$_n$, involving the sorting out of one pair out of four. In the case of π salt, the insertion of the enantiomeric pair of this impurity (ν or ν′) leads to level $x + 1$ with π′ pair at the top. Thus both ions have the wrong absolute configuration and the desorption of this impurity *via* F0D2 is compulsory. But in the case of the racemic compound (Organisation chart 4), the insertion of the enantiomeric pair of the impurity (π or π′), directly leads to level $x + 2$, whereby the crystal growth *via* simple adsorption of the right pairs can go on. So, the desorption of a wrong π or π′ pair from the top of the IPBC *via* F0D2 is not necessary any more (the insertion of the enantiomeric pair *via* F3D1 is sufficient). The racemic compound is still kinetically favoured with regard to the activation energies of the possible desorption mechanisms occurring when a wrong pair is adsorbed at the top of an IPBC. Moreover, the racemic compound is still favoured in terms of diffusion parameters since the free migration path of a wrong pair can still be limited to

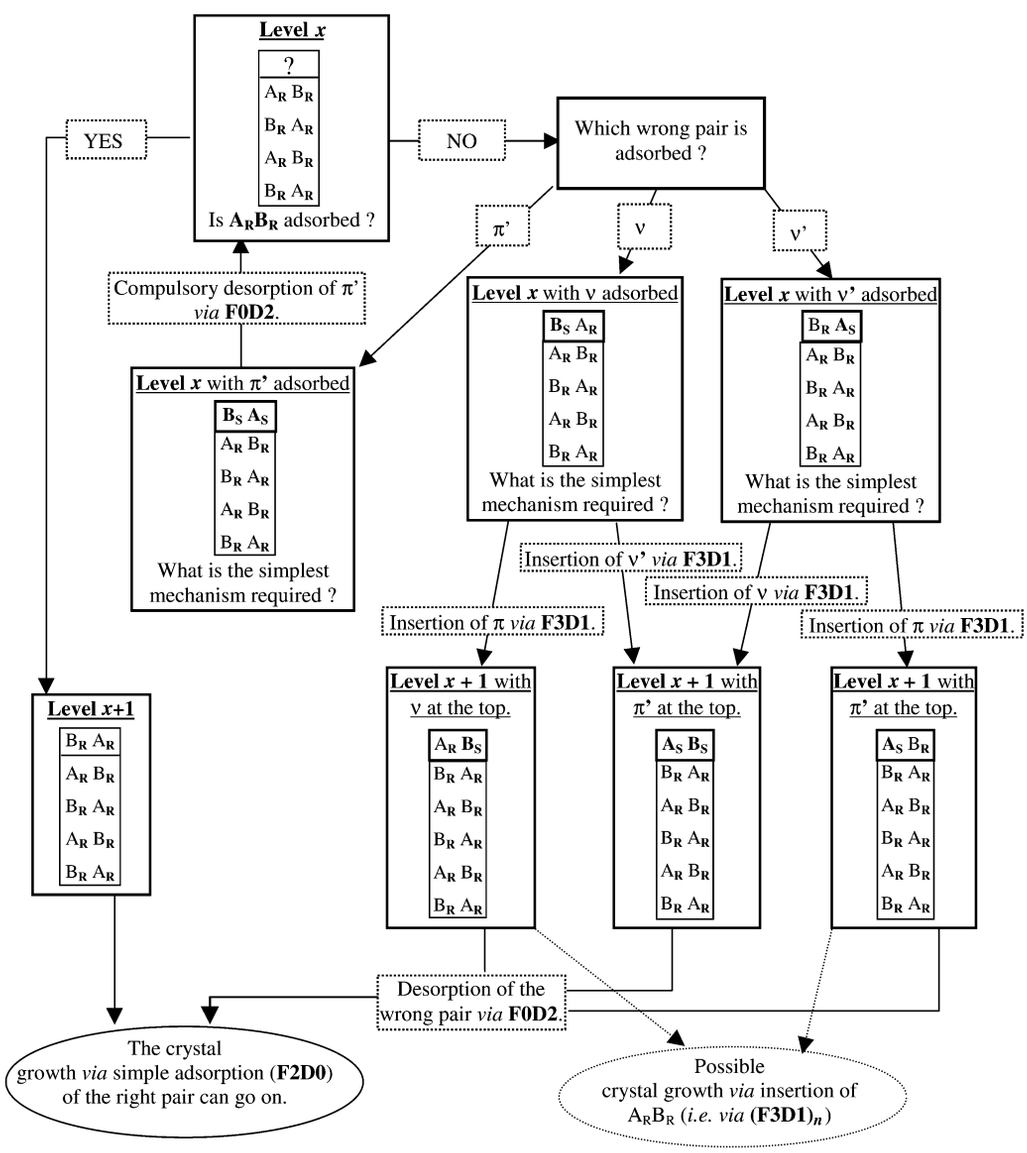


**Organisation chart 3** Crystal growth of the conglomerate in the case of a chiral counter ion.

the distance between two neighbouring IPBCs, whereas a π′ pair desorbed from the π salt crystal surface should migrate to a π′ salt crystal.

In both cases (chiral and non-chiral counter ion), the crystallisation of the racemic compound is kinetically favoured, but these organisation charts are not sufficient to determine whether this kinetic advantage of the racemic compound is greater when the counter ion is chiral. A different development of the model is used to answer this question.

Crystals grow by means of successive adsorption, insertion and desorption mechanisms called "events". At the top of an IPBC, these events occur randomly, depending on the nature of the ion pairs migrating at the vicinity of the surface, depending on local energy and/or matter accumulation (the former allowing the activation of these mechanisms) caused by thermal or mechanical motion. Therefore, if we still consider the crystal growth of a perfect crystal, the number of rungs formed for a given number of events *i* will depend on the order and the nature of these successive mechanisms, that is to say, on the "crystal growth path". Thus, it is interesting to determine both the outcome (*i.e.* the number of rungs formed) and the probability of each possible crystal growth path, for a given *i*, by means of tree diagrams.

The assumptions used for the construction of the organisation charts remain; particularly, F3D1 is a highly discriminating mechanism so that only a pair containing the ion of required absolute configuration can be inserted in the course of a F3D1 mechanism. If the approaching pair does not contain this appropriate ion, it results in a F0D2 mechanism of the wrong pair adsorbed. F0D2 is then the consequence of F3D1 failure, so that the desorption of a right pair is not considered in this model. Thus, at each step, only efficient mechanisms are envisaged, *i.e.* the mechanisms which make a perfect crystal grow or allow the return to a situation where the crystal growth of a perfect crystal is possible when a wrong pair is adsorbed. In any case (conglomerate or racemic compound, with chiral counter ion or not) a synthetic table can substitute for the tedious tree diagram. These tables (hereafter called "triangular tables") are constructed in a recurrent way and it is therefore much easier to increase the number of events *i*.

Other notations must be defined: we still consider a ladder from which *x* rungs are already formed. This ladder is designated by a number and a letter between parentheses. The number represents the number of rungs formed. The letter symbolises the nature of the pair at the top: *A* if the absolute configuration of the ion(s) is (are) that required; *Z* if the absolute configuration of the ion(s) is (are) not that required; *M* or *N* if only one among both chiral ions at the top has not the required absolute configuration. Thus the initial state is (0*A*).

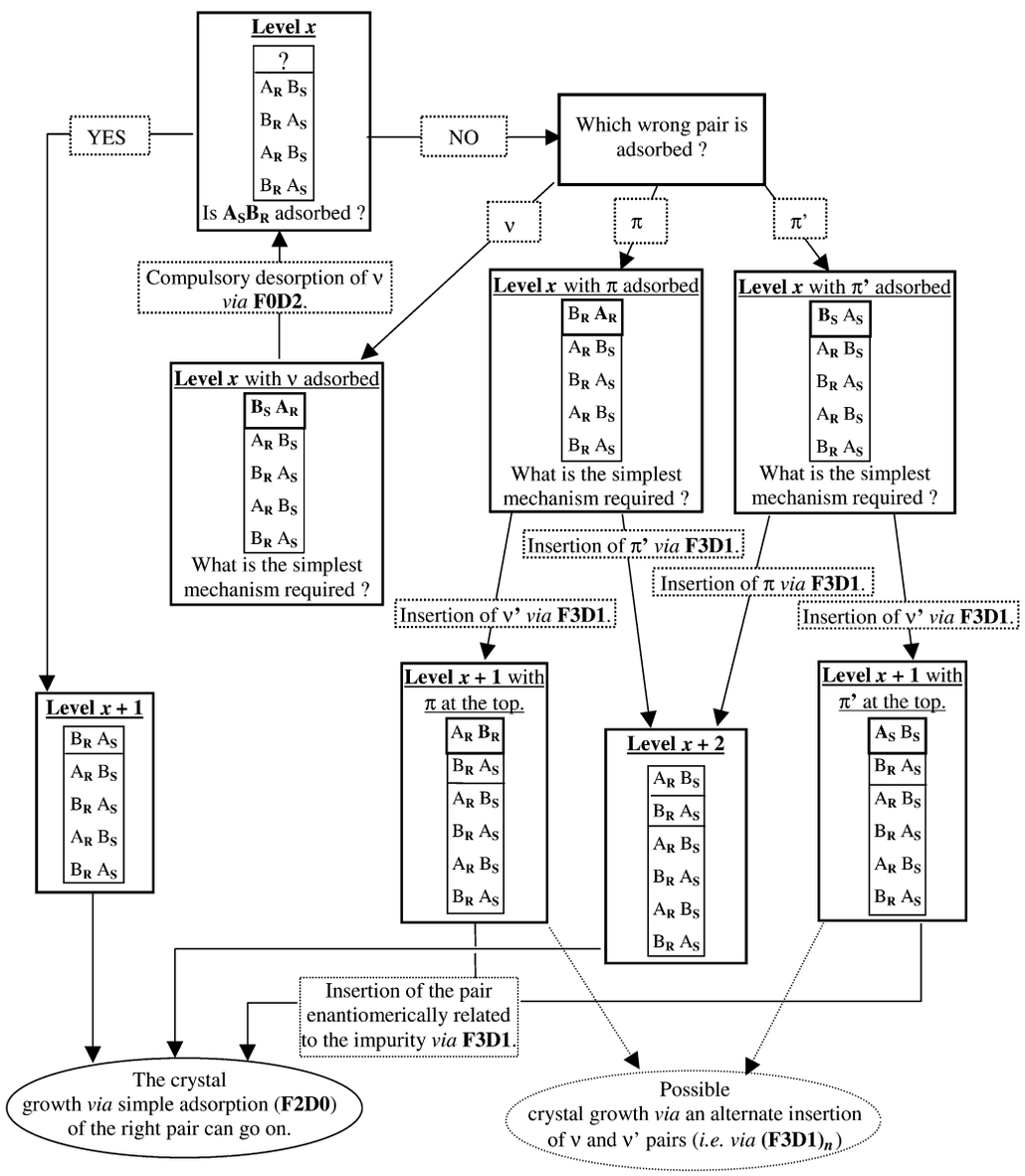


**Organisation chart 4** Crystal growth of the ν-type racemic compound in the case of a chiral counter ion.

**Table 7** The possible situations of the ladder are preceded by the sum of the probabilities of all the paths leading to these situations. For instance, when 4 events occurred, the formation of 2 rungs with the right one at the top (2*A*) has a probability of 3/8th (6 crystal growth paths of 1/16th probability each (see Fig. 7))

| | *j* | | | | |
|---|---|---|---|---|---|
| Number of events *i* | 1 | 2 | 3 | 4 | 5 |
| 0 | 1 (0*A*) | | | | |
| 1 | 1/2 (1*A*) | 1/2 (1*Z*) | | | |
| 2 | 1/4 (2*A*) | 1/2 (2*Z*) | 1/4 (0*A*) | | |
| 3 | 1/8 (3*A*) | 3/8 (3*Z*) | 3/8 (1*A*) | 1/8 (1*Z*) | |
| 4 | 1/16 (4*A*) | 1/4 (4*Z*) | 3/8 (2*A*) | 1/4 (2*Z*) | 1/16 (0*A*) |

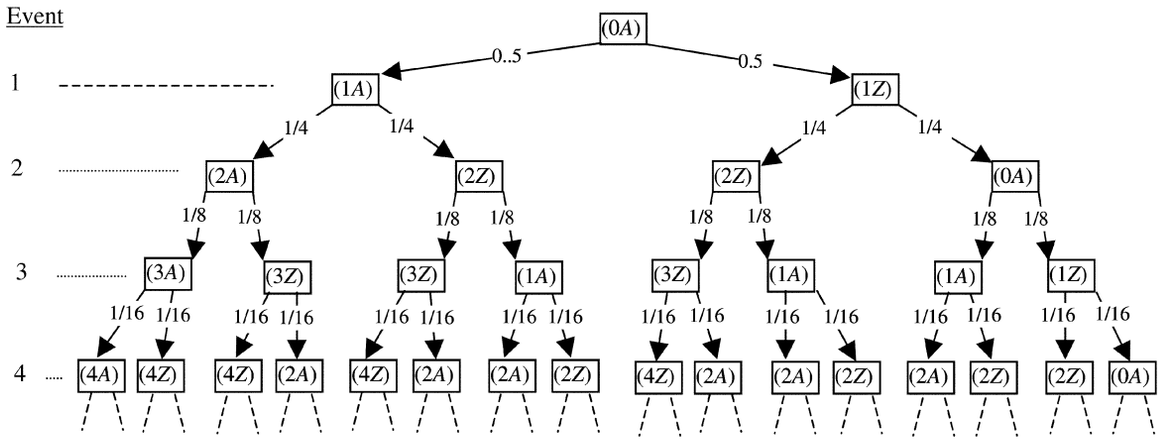


**Fig. 7** Tree diagram of all the possible "crystal growth paths" after 4 events in the case of the conglomerate with NCCI. The probability of each crystal growth path (on the arrows) precedes the obtained situation of the ladder [*i.e.* the number of rungs formed and the absolute configuration of the ion pair at the top (*A* or *Z* according to the notations introduced before in the main text)].

*Developed case (conglomerate with non-chiral counter ion (NCCI); Fig. 7, Table 7 and Scheme 8).* The simplest case is depicted here but the difficulty increases in the case of a CCI, and particularly with a non-racemic solution (calculation detailed in the electronic supplementary information).


**Scheme 8** Possible evolutions of an IPBC (with their probabilities) in the case of the conglomerate with NCCI, depending on the configuration (*A* or *Z*) of the ion pair at the top.

(i) Either the chiral ion of the pair at the top has the right absolute configuration (*A*); in that case, the possible events are: the adsorption of the right enantiomer (noted $+1A$ because one rung is formed and a right pair is at the top after the adsorption); the adsorption of the wrong enantiomer (noted $+1Z$ because one rung is formed but a wrong pair is at the top). Since both enantiomers grow at the same rate from a racemic solution, the proportion of both enantiomers in the mother liquor remains 0.5 and the probability of each event is 0.5.

(ii) Or the chiral ion of the pair at the top has the wrong absolute configuration (*Z*) and the two possible events are: the insertion of the right pair *via* F3D1 (noted $+1Z$ because one additional rung is formed and a wrong pair remains at the top) (see Organisation chart 1); the desorption of this wrong pair (noted $-1A$ because one rung is removed and a right pair at the top is retrieved). The probability of each event is still 0.5.

The tree diagram (Fig. 7) is made up of two elementary branches (Scheme 8). Table 7 is an easier way of presenting the same results. Let $i = 0, 1, 2, \ldots n$ be the rows of the table, $j = 1, 2, 3, \ldots m$ be the columns and $U_{i,j}$ be the probability of reaching the situation corresponding to the column $j$ when $i$ events occurred. It appears from Scheme 8 that a situation ($xZ$) can be obtained from the situations ($x - 1A$) and ($x - 1Z$) with a probability of 0.5 each, so that $U_{i,j} = 0.5\ U_{i-1,j-1} + 0.5\ U_{i-1,j}$ $\forall i$, $\forall j$ even (Table 7), if we consider that $U_{i,j} = 0$ in undefined cells ($U_{i,0}$, $U_{3,5}$ for instance). A situation ($xA$) can be obtained from the situations ($x - 1A$) and ($x + 1Z$) with a probability of 0.5 each, so that $U_{i,j} = 0.5U_{i-1,j-1} + 0.5U_{i-1,j}$ $\forall i$, $\forall j$ odd. Finally, only eqn. (6) is necessary to construct the Table 7. Thus the probability of each possible situation ($U_{i,j}$) can be calculated whatever the number of events $i$ (*i.e.* for each row). It is interesting to notice (from Fig. 7 and Scheme 8) that an odd number of rungs are formed when an odd number of events occurred. In the same way, only an even number of rungs can be formed for an even number of events. Thus, considering $i$ events, the various numbers of rungs formed can be expressed as $i - 2q$ where $q$ is an integer ranging from 0 to $i/2$. In accordance with the statement above, $i - 2q$ and $i$ have the same parity. $P_{i-2q}$ is the sum of the probabilities ($U_{i,j}$) of the crystal growth paths leading to the formation of $i - 2q$ rungs ($0 \le q \le i/2$, $q$ integer) whatever the nature of the pair at the top (only the situations ($i - 2qA$) and ($i - 2qZ$) in this simple case). Obviously, for a given number of events $i$, the sum of the probabilities $P_{i-2q}$ for $q = 0$ to $q = i/2$ ($\Sigma P_{i-2q}$) equals 1. Let's define $E = (i - 2q)/i$ as the percentage of rungs formed (*i.e.* the ratio number of rungs formed ($i - 2q$) by the number of rungs formed if each event is the adsorption of the right pair ($i$)). When $P_{i-2q}$ is plotted against $E$ for different values of $i$, gaussian-type curves are obtained. For the conglomerate with NCCI, the maximum of each curve is obtained for $E(P^{\max}_{i-2q}) = 50\%$ (Fig. 8).

$$U_{i,j} = 0.5U_{i-1,j-1} + 0.5U_{i-1,j}\ \forall i,\ \forall j \qquad (6)$$

$\Delta E$ is defined as the interval of $E$, centred on $E(P^{\max}_{i-2q})$, for which the sum of the values $P_{i-2q}$ ($\Sigma P_{i-2q}$) is greater than 0.99. This interval $\Delta E$ decreases when $i$ increases; this can be confirmed by plotting $P_{i-2q}/(P^{\max}_{i-2q}) = f(E)$ for increasing values of $i$ (Fig. 9). The maximum of the gaussian peak remains 1 and the

**Table 8** Comparison of the results obtained in the four cases (conglomerate and racemic compound with NCCI or CCI)

| | Non-chiral counter ion (NCCI) | | Chiral counter ion (CCI) | |
|---|---|---|---|---|
| | Conglomerate | Racemic compound | Conglomerate | Racemic compound |
| Most probable percentage of rungs formed $E(P^{\max}_{i-2q})$ (%) | 50.0 | 66.7 | 28.0 | 39.1 |
| Relative advantage of the racemic compound RA (%)[a] | +33.3 | | +39.6 | |
| $\Delta E$ (%) ($\Sigma P_{i-2q}$ (%))[b] | 2.56 (99.01) | 3.28 (99.02) | 2.20 (99.00) | 3.28 (99.05) |

[a] $RA = 100[E(P^{\max}_{i-2q})_{\mathbf{rac}} - E(P^{\max}_{i-2q})_{\mathbf{conglo}}]/E(P^{\max}_{i-2q})_{\mathbf{conglo}}$. [b] Values obtained for 10000 events.

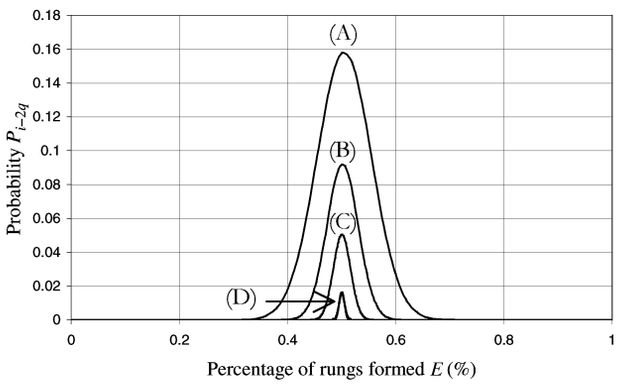


**Fig. 8** Graph $P_{i-2q} = f(E)$ in the case of the conglomerate with NCCI, for $i$ = 100 (A), 300 (B), 1000 (C) and 10000 (D) events.

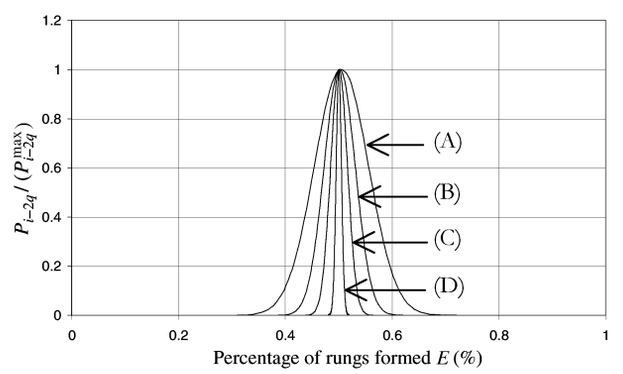


**Fig. 9** The curves obtained for 100 (A), 300 (B), 1000 (C) and 10000 (D) events are normalised by plotting $P_{i-2q}/(P^{\max}_{i-2q}) = f(E)$. The maximum is brought to 1 and $\Delta E$ decreases when $i$ increases.

interval $\Delta E$ decreases when $i$ increases. The number of rungs formed tends towards $E(P^{\max}_{i-2q})$ when $i$ increases.

Therefore, the more $i$ increases, the more probable the formation of $i/2$ rungs.

*The three other cases.* In the three other cases (racemic compound with NCCI, conglomerate and racemic compound with CCI), the elementary branches of the tree diagrams (and therefore the corresponding triangular tables) are different (see the case of the conglomerate with CCI in Scheme 9). However, the graphs $P_{i-2q} = f(E)$ are also gaussian-type curves whose interval $\Delta E$ decreases when $i$ increases. The difference lies in the values of $E(P^{\max}_{i-2q})$ *i.e.* in the most probable percentage of rungs formed (Table 8).

Several conclusions can be drawn from these results: (i) the faster crystal growth of a racemic compound whatever the nature of the counter ion (chiral or not) is confirmed since the number of rungs formed for a given number of events is larger; (ii) within the framework of the hypotheses of this model, the kinetic advantage of the racemic compound is greater with a CCI. For a given $i$, the percentage of rungs formed in the case of the racemic compound ($E(P^{\max}_{i-2q})_{\mathbf{rac}}$) is 39.6% greater than $E(P^{\max}_{i-2q})_{\mathbf{conglo}}$ whereas it is only 33.3% greater with an NCCI; (iii) one can note that for a given number of events $i$, the width of the peaks obtained for the racemic compounds (CCI and NCCI) is greater. It means that the probabilities of crystal growth paths leading to the values around $E(P^{\max}_{i-2q})$, are greater for the racemic compounds than for the conglomerates. According to the evolution of the curves, this difference may become negligible when $i$ increases.

### Supersaturation capacity of the mother solutions

A chiral counter ion leads to four components in the solution (instead of 2 or 3 during the usual PC of respectively covalent or ionic [with NCCI] compounds). Consequently, according to this model, the presence of this additional component hinders the processes involved in the crystal growth of these salts. However, crystallisation starts by a nucleation step which consists of molecular aggregation processes leading to the formation of nuclei up to a critical size where growth can start. The configuration of the nuclei is akin to the crystal structure so that we may assume that at least ill-assembled ladder shaped IPBCs must form during this stage. Nucleation kinetics are controlled by interfacial energies (important role of solvent, impurities, structural defaults (dislocations) for example). However, this model, describing the self-assembling processes of the crystallising units, might be an additional factor acting upon nucleation kinetics. From this point of view, the poor efficiency of the more probable successions of basic mechanisms, in the case of CCI, may also account for a slower primary nucleation and therefore account for the observed increased supersaturation capacity of the mother solution (a saturated solution of (±)-**1**–(±)-**2** in ethanol at 22.7 °C ($c_{\mathbf{sat,22.7\,°C}} = 17.5\%$) remains homogeneous during at least 1 h at 7 °C ($c_{\mathbf{sat,7\,°C}} = 12.8\%$, $\beta = 1.4$)).

So, (i) a larger supersaturation is required to elicit the crystallisation of the conglomerate with CCI; (ii) a greater relative advantage of the nucleation and crystal growth rates of the racemic compound is expected in the case of CCI. Therefore, a third conclusion can be inferred from both of these: the detection of an unstable or metastable racemic compound is expected to be easier in a reciprocal ternary system of diastereomeric salts than in a simple binary system of chiral salts with NCCI.

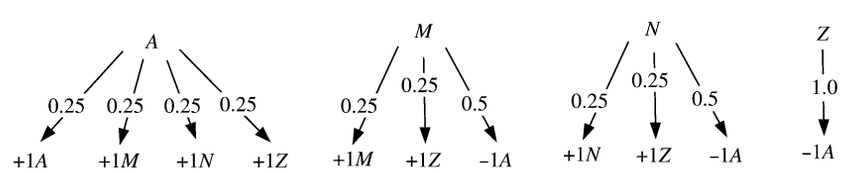


**Scheme 9** Possible evolutions of an IPBC (with their probabilities) in the case of the conglomerate with CCI, depending on the configuration ($A$, $M$, $N$ or $Z$) of the ion pair at the top. (The way this scheme is obtained is detailed in the electronic supplementary information.)

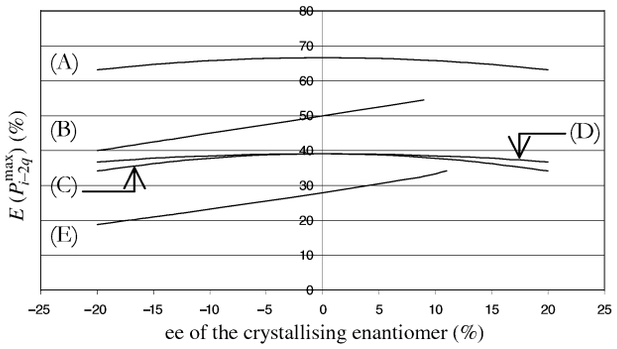


**Fig. 10** Evolution of $E(P_{i-2q}^{max})$ with respect to the ee of the mother liquor (a negative ee stands for an excess of the counter enantiomer). NCCI rac (A), NCCI enantiomer (B), CCI π-type rac (C), CCI ν-type rac (D) and CCI enantiomer (E). (A), (C) and (D) curves display an axial symmetry with reference to ee = 0%.

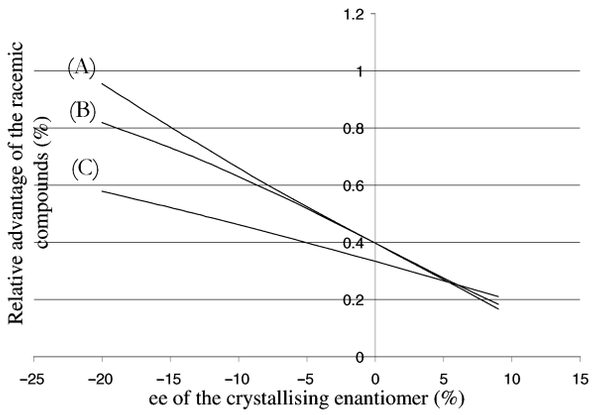


**Fig. 11** Evolution of the relative kinetic advantage of the racemic compound with respect to the ee of the mother liquor (a negative ee stands for an excess of the counter enantiomer). CCI ν-type racemic compound (A), CCI π-type racemic compound (B) and NCCI (C).

### Application to the preferential crystallisation

During the PC, the mother liquor is not racemic any more but is initially enantiomerically enriched and the excess of the crystallising enantiomer decreases until the non-crystallising enantiomer becomes predominant in the mother liquor. As a consequence, the probability of existence of each pair in the mother liquor and therefore the probabilities of each possible mechanism in Scheme 8 evolve in the course of the crystallisation and therefore during the construction of the tree diagram (or the corresponding triangular table). In order to bypass this difficulty, we determined the triangular tables for given values of ee (and therefore for given values of probabilities). It is implicitly assumed that the percentage of rungs formed $E(P_{i-2q}^{max})$ could have been reached with a small $\Delta E$, without any significant change of the ee of the solution (and therefore of the probability of each mechanism).

**Case of NCCI.** Each value of ee corresponds to a proportion of both enantiomers in the mother liquor. This composition determines the values of the probabilities of each mechanism in the different configurations *A* or *Z* of the ion pair at the top.

**Case of CCI.** The proportion of each pair in the mother liquor must be determined with respect to the ee. As no chiral discrimination occurs in the solution, we assume that the probability of existence of each pair was 0.25 in the racemic solution. Therefore we implicitly assumed that the equilibrium constant of the double decomposition reaction (1) was $K = 1$. This equilibrium is used to determine the proportion of each pair in the mother solution when ee ≠ 0.

As the PC is an out of equilibrium process, another assumption arose. The kinetics of the homogeneous equilibrium of double decomposition must be faster than the kinetics of crystallisation, so that the proportions of each pair, calculated on the basis of this chemical equilibrium are actually observed in the mother liquor during the PC. This can be argued as follows: there is no sterical difficulty in exchanging the counter ions of two ion pairs in solution (*i.e.* by contrast to the crystallisation mechanisms at the crystal surfaces, an ion pair can bump another one from any direction of the 3D space and there are no docking constraints).

Thus, peaks are still obtained for $P_{i-2q} = f(E)$ curves. In both cases (CCI and NCCI), the values of $E(P_{i-2q}^{max})$ are determined for several values of ee (Fig. 10). Then the relative advantage $(RA = [E(P_{i-2q}^{max})_{rac} - E(P_{i-2q}^{max})_{conglo}]/E(P_{i-2q}^{max})_{conglo})$ is calculated for these ee. Both cases of ν-type and π-type racemic compounds are envisaged for the CCI but only a small difference is observed so that the same conclusion can be drawn (Fig. 11; the way this figure is obtained is detailed in the electronic supplementary information): in both cases, the kinetic advantage of the racemic compound increases all along the PC (from 5 to −15% ee in the mother liquor in the most favourable cases). Moreover this kinetic advantage is greater and increases faster when the counter ion is chiral. This result emphasises the interest of the AS3PC process in the case of the simultaneous resolution of this kind of acid and base: the auto-seeding and the adapted cooling program provide a full control on the crystal growth (*via* the presence of a large amount of crystals ready for growth at the onset of the crystallisation and the continuous control of the supersaturation),[2b,c] so that a putative unstable (or metastable) racemic compound is less likely to crystallise during the PC.

## Conclusion and prospect

Although re-examination of the reciprocal ternary system of (±)-**1** and (±)-**2** confirms the presence of a stable conglomerate of p and p′ salts with no detectable solid solution, a high temperature form of n salt (called n salt form II) as well as an unstable racemic compound have been detected. Kinetic parameters of the irreversible solid–solid transition of this unstable racemic compound into the stable conglomerate were determined by means of high temperature XRPD analyses. The simultaneous resolution of (±)-**1** and (±)-**2** by means of preferential crystallisation (AS3PC) of the stable pair of salts (p–p′) in ethanol is achieved at a two litre scale (13 consecutive runs). Different crystallisation conditions (cooling program, stirring rate, crystallisation duration) were tested but the magnitude of the entrainment effect (given by the maximum ee of the mother liquor at the end of the process) was limited to 5.2%. This intrinsic limit is consistent with the existence of an unstable racemic compound, as proposed in the model of molecular interactions occurring at the crystal–mother solution interface in the course of preferential crystallisation.[7] In order to give a realistic view of the kinetics in competition, an extension of this model is proposed. It involves the following hypotheses: the crystal structures are composed of ladder-shaped IPBCs, perfect crystals are growing, three basic mechanisms called events (adsorption F2D0, desorption F0D2 and insertion F3D1), involving ion pairs only, are considered. According to the way they follow one another, a given number of events *i* results in a given number of rungs formed. In each case (conglomerate, racemic compound, chiral counter-ion, non-chiral counter-ion), the more *i* increases, the more probable a given percentage of rungs formed $E(P_{i-2q}^{max})$. The $E(P_{i-2q}^{max})$ values obtained in each case are: conglo-CCI (28%)–rac-CCI (39%)–conglo-NCCI (50%)–rac-NCCI (67%). It appears from these values that the racemic compound with CCI is more kinetically favoured (with a relative advantage $(RA = [E(P_{i-2q}^{max})_{rac} - E(P_{i-2q}^{max})_{conglo}]/E(P_{i-2q}^{max})_{conglo})$ of 39.6%) than the racemic compound with NCCI (RA = 33.3%). Therefore, an easier detection of unstable

or metastable racemic compounds is expected in reciprocal systems of diastereomeric salts. According to the hypotheses postulated and particularly to the number of parameters acting upon the crystal growth and nucleation rates but not taken into account in this model, these values provide only crystal growth and nucleation kinetics trends.

In both cases, as the proportion of the right crystallising enantiomer decreases in the mother liquor during the PC, the relative advantage of the racemic compounds increases. This relative advantage is greater and increases faster with the CCI so that the full control on crystal growth provided by the AS3PC process[2b,c] is of prime importance to perform the simultaneous resolution by PC in such reciprocal systems where unstable or metastable racemic compounds are expected to be widely kinetically favoured.

The work ahead consists in investigating other couples of racemic acid and base in order to: (i) check the general feasibility of the simultaneous resolution *via* preferential crystallisation of the stable pair of reciprocal salts in the case of stable conglomerates; (ii) confirm the expected limited performances of the preferential crystallisation when an unstable or metastable racemic compound is detected. However, an in-depth question remains: does the increased number of chiral species in reciprocal ternary systems of racemic acid and base penalise the formation of stable racemic compounds? In other words, is the 5 to 10% proportion of stable conglomerates observed in the case of binary systems of simple racemic mixtures of ionic (with NCCI) or covalent compounds increased in such reciprocal systems?

## Experimental

### Instruments used

The crystalline phases were characterised by means of a Setaram Differential Scanning Calorimeter 141 and an automatic diffractometer Siemens D-5005 using the Cu $K\alpha_1$ radiation. The peak assignment of the XRPD patterns was performed by using the DICVOL 91 software.[14] Optical rotations were measured by means of a Perkin-Elmer 241 polarimeter. Refractive indexes were determined by means of an OPL refractometer using an Na lamp.

### Polarimetry

The solutions were prepared as follows: in a 2 ml gauged flask, 15–20 mg of dried solid was accurately weighed and dissolved in ethanol. As the optical rotation of pure p salt ($\alpha°$) does not linearly depend on the mass of dissolved salt,[4] a calibration was carried out. $\alpha°$ values of solutions containing different masses ($m$) of pure p salt were measured. $\alpha°$ was given by the equation $\alpha° = 0.0452 \times m^{0.818}$. OP was given by $\alpha/\alpha°$.

### Solubility measurements

The solubilities of the conglomerate of p and p′ salts in ethanol were determined by the following procedure: in a stopped glass thermostatted tube, a previously homogenised solution of an equimolar mixture of (±)-**1** and (±)-**2** was cooled down to 0 °C under vigorous magnetic stirring, in order to obtain particles as small as possible. Then the slurry was heated up to and maintained at the required temperature under a magnetic stirring for at least 48 hours. After sedimentation the solution was slowly pipetted and weighed in a stopped flask previously tared. The solvent was evaporated at room temperature and the residue was weighed. The mass of the residue divided by the mass of the pipetted solution gave the mass percent solubility of the solute. The crystalline phase in equilibrium with the mother solution was filtered off and checked by means of an XRPD analysis.

### AS3PC experiments

(±)-**1** and (±)-**2** were distilled under vacuum before use. All the experiments were carried out with absolute ethanol. Preferential crystallisation was carried out in a thermostatted two litre double inner wall crystalliser. A mechanical stirring was ensured by means of a corrugated rectangular shaped (7–9 cm) paddle drilled with three 1 cm diameter holes. The filtration device was a thermostatted two litre double inner wall glass filter No. 3.

**Concentration and ee determinations.** *Notations and definitions.* The pure enantiomorphous p salt, p′ salt and their racemic mixture are symbolised by (++), (−−) and (±±) respectively.

$m_{(++)}$, $m_{(--)}$ and $m_S$ are the masses of p salt, p′ salt and solvent respectively.

The total mass of the mother solution is given by eqn. (7).

$$m_T = m_{(++)} + m_{(--)} + m_S \quad (7)$$

The mass of the enantiomorphous salt in excess in a non-racemic mother solution is given by eqn. (8).

$$m_{ee} = |m_{(++)} - m_{(--)}| \quad (8)$$

The mass of racemic mixture in the solution is given by eqn. (9).

$$m_{(\pm\pm)} = m_{(++)} + m_{(--)} - m_{ee} \quad (9)$$

The total mass% concentration of both enantiomorphous salts is given by eqn. (10).

$$c_T = 100\,(m_{(++)} + m_{(--)})/m_T \quad (10)$$

The mass% concentration of the racemic mixture in the mother solution, neglecting the mass of the ee in the total mass of the system, is given in eqn. (11).

$$c(\pm\pm) = (100m_{(\pm\pm)})/(m_{(\pm\pm)} + m_S) \quad (11)$$

The enantiomeric excess (%) of the mother solution is given in eqn. (12).

$$\text{ee} = (100m_{ee})/(m_T - m_S) \quad (12)$$

$\alpha$ is the optical rotation of the neat mother solution, measured at 20.2 °C and 365 nm wavelength.

$n$ is the refractive index of the mother solution at 20.2 °C measured with the D line of an Na lamp.

*The calibration method.* The aim was to determine the ee of the mother solution in the course of the preferential crystallisation, by means of optical rotation ($\alpha$) and refractive index ($n$) measurements. The problem was the following: even if $n$ gives directly $c_T$ *via* eqn. (13), the ee could not be directly deduced

$$n = 1.75 \times 10^{-3}\, c_T + 1.36 \quad (13)$$

from $\alpha$ since it depends on the value of $c(\pm\pm)$. Therefore, a specific method was developed: a series of 16 solutions with values of $c_T$, $c(\pm\pm)$ and ee in the range of those expected in the mother solution in the course of the preferential crystallisation, were prepared. Namely, for each $c(\pm\pm) = 15.5$, 16.5, 17.5 and 18.5%, four solutions with ee = 0, 2, 4, 6% were prepared. $\alpha$ and $n$ of each solution were measured. By plotting $\alpha$ *versus* ee for each value of $c(\pm\pm)$, four segments of line [eqn. (14)] were

$$\alpha = a_{c(\pm\pm)} \times \text{ee} \quad (14)$$

obtained. The slopes of these segments linearly depended on $c(\pm\pm)$ according to eqn. (15), so that eqn. (16) holds. On the other hand, eqn. (17) was determined from eqns. (11), (9), (10),

$$a_{c(\pm\pm)} = b \times c(\pm\pm) + d \quad (15)$$

$$\text{ee} = a/(b \times c(\pm\pm) + d) \quad (16)$$

$$c(\pm\pm) = (100 - \text{ee})/((100/c_T) - \text{ee}) \quad (17)$$

(12) and (7). Thus from eqn. (16) and (17), a quadratic equation with $c(\pm\pm)$ as unknown was obtained and resolved by means of the discriminant method. The final equation [eqn. (18)] with $\Delta$ given by eqn. (19) allowed us to determine $c(\pm\pm)$ from $a$ and $c_T$ (directly obtained from *n via* eqn. (13)) and therefore to deduce ee from eqn. (16).

$$c(\pm\pm) = ([c_T(a + b) - d] + \Delta^{0.5})/2b \quad (18)$$

$$\Delta = [d - c_T(a + b)]^2 + 4b(d - a)c_T \quad (19)$$

**Recrystallisation of crude crops.** The crystals were dissolved in a minimum quantity of hot ethanol. Four volumes of toluene were gently added to the hot solution. Then, the clear solution was allowed to slowly cool down to room temperature without any stirring. A spontaneous nucleation occurred during the cooling. Then, the suspension was magnetically stirred at room temperature for at least 24 h. The crystals were filtered off on the 2 L glass filter No. 3 by means of $N_2$ pressure, then washed with DIPE and dried at 75 °C for 1 h.

**Salting out of pure salts.** To 60 g of pure salt, 40 ml $H_2O$, 150 ml toluene and 25 ml HCl 37% were respectively added under stirring. Then the aqueous phase was extracted, washed with 150 ml of toluene. The organic phases were mustered, washed with 25 ml $H_2O$ and dried with $MgSO_4$. The toluene was evaporated under vacuum.

## Acknowledgements

ACROS ORGANICS is gratefully acknowledged for supplying starting racemic mixtures. Thanks are also due to Dr Pascal Cardinael for HPLC analyses.

## References

1 (*a*) E. Eliel, S. H. Wilen and L. N. Mander, *Stereochemistry of Organic Compounds*, Wiley-Interscience, New York, 1994; (*b*) J. Jacques, A. Collet and S. H. Wilen, *Enantiomers, Racemates and Resolutions*, Kriger Publishing Company, Malabar, Florida, 1994; (*c*) P. Newman, *Optical Resolution Procedures for Chemical Compounds*, Optical Resolution Information Center, New York, 1981.
2 (*a*) G. Coquerel, M.-N. Petit and R. Bouaziz, EP 0720.595 B1/1995 (*Chem. Abstr.*, 1995, **123**, 255843c); (*b*) E. Ndzié, P. Cardinael, A.-R. Schoofs and G. Coquerel, *Tetrahedron: Asymmetry*, 1997, **8 (17)**, 2913; (*c*) S. Beilles, P. Cardinael, E. Ndzié, S. Petit and G. Coquerel, *Chem. Eng. Sci.*, 2001, **56**, 2281.
3 (*a*) Y. Takahashi, K. Arai, Y. Obara, H. Matsumoto and S. Tsuchiya, Jpn. Kokai Tokkyo Koho JP 61,134,344, 1986 (*Chem. Abstr.*, 1987, **106**, 32591s); (*b*) C.-H. Wong and K.-T. Wang, *Tetrahedron Lett.*, 1978, **40**, 3813; (*c*) T. Shiraiwa, M. Nagata, K. Kataoka, Y. Sado and H. Kurokawa, *Nippon Kagaku Kaishi*, 1989, 84 (*Chem. Abstr.*, 1989, **110**, 212673m); (*d*) H. Nohira, H. Fujii, M. Yajima and R. Fujimura, Eur. Pat. Appl. EP 30, 871, 1981 (*Chem. Abstr.*, 1982, **96**, 34875m); (*e*) T. Shiraiwa, M. Morita, K. Iwafugi and H. Kurokawa, *Nippon Kagaku Kaishi*, 1983, 1743 (*Chem. Abstr.*, 1984, **100**, 175181v).
4 M. Leclercq and J. Jacques, *Bull. Soc. Chim. Fr.*, 1975, 2052.
5 M. Leclercq, J. Jacques and R. Cohen-Adad, *Bull. Soc. Chim. Fr.*, 1982, 388.
6 M.-C. Brianso, *Acta Crystallogr., Sect. B*, 1976, **32**, 3040.
7 S. Houllemare-Druot and G. Coquerel, *J. Chem. Soc., Perkin Trans. 2*, 1998, 2211.
8 (*a*) H. Eyring, *J. Chem. Phys.*, 1935, **3**, 107; (*b*) W.-F.-K. Wynne-Jones and H. Eyring, *J. Chem. Phys.*, 1935, **3**, 492.
9 O. Monnier, G. Fevotte, C. Hoff and J. P. Klein, *Chem. Eng. Sci.*, 1997, **52 (7)**, 1125.
10 (*a*) M. Simonyi, *Problems and Wonders of Chiral Molecules*, 1990, p. 91 (article by A. Collet); (*b*) M. R. Caira, R. Clauss, L. R. Nassimbeni, J. L. Scott and A. F. Wildervanck, *J. Chem. Soc., Perkin Trans. 2*, 1997, 763; (*c*) K. Kinbara, Y. Hashimoto, Y. Sukegawa, H. Nohira and K. Saigo, *J. Am. Chem. Soc.*, 1996, **118**, 3441; (*d*) K. Kinbara, Y. Kobayashi and K. Saigo, *J. Chem. Soc., Perkin Trans. 2*, 1998, 1767.
11 (*a*) P. Hartman and W. G. Perdock, *Proc. K. Ned. Akad. Wet. Ser. B: Palaeontol. Geol. Phys. Chem.*, 1952, **55**, 134; (*b*) P. Hartman and W. G. Perdock, *Acta Crystallogr.*, 1955, **8 (49)**, 521; (*c*) P. Hartman, *Crystal Growth: An Introduction*, ed. P. Hartman, North-Holland, Amsterdam, 1981, p. 367.
12 M. Hillert, *Phase Equilibria Phase Diagrams and Phase Transformations. Their Thermodynamic Basis*, Cambridge University Press, 1998, ISBN 0 521 56270 8 Hardback, ISBN 0 521 56584 7 Paperback.
13 X. Y. Liu, E. S. Boek, W. J. Briels and P. Bennema, *Nature*, 1995, **374**, 342.
14 D. Louer and M. Louer, *J. Appl. Crystallogr.*, 1972, **5**, 271; A. Boultif and D. Louer, *J. Appl. Crystallogr*, 1991, **24**, 987.